Received: 6 May 2022 | Accepted: 7 June 2022

DOI: 10.1002/dro2.11

RESEARCH ARTICLE

Droplet WILEY

Pneumatic programmable superrepellent surfaces

Songtao Hu[1] | Xiaobao Cao[2] | Tom Reddyhoff[3] | Xijia Ding[1] | Xi Shi[1] | Daniele Dini[3] | Andrew J. deMello[4] | Zhike Peng[1] | Zuankai Wang[5]

[1]School of Mechanical Engineering, State Key Laboratory of Mechanical System and Vibration, Shanghai Jiao Tong University, Shanghai, China

[2]Guangzhou Laboratory, Guangzhou, China

[3]Department of Mechanical Engineering, Imperial College London, London, UK

[4]Department of Chemistry and Applied Biosciences, ETH Zurich, Zurich, Switzerland

[5]Department of Mechanical Engineering, City University of Hong Kong, Hong Kong, China

Correspondence
Songtao Hu, School of Mechanical Engineering, Shanghai Jiao Tong University, Shanghai 200240, China.
Email: hsttaotao@sjtu.edu.cn

Funding information
National Natural Science Foundation of China, Grant/Award Numbers: 12002202, 12121002; Young Elite Scientist Sponsorship Program by the China Association for Science and Technology, Grant/Award Number: YESS20200403; State Key Laboratory of Mechanical System and Vibration, Grant/Award Number: MSVZD202104

Abstract

Morphological transformation of surface structures is widely manifested in nature and highly preferred for many applications such as wetting interaction; however, in situ tuning of artificial morphologies independent of smart responsive materials remains elusive. Here, with the aid of microfluidics, we develop a pneumatic programmable superrepellent surface by tailoring conventional wetting materials (e.g., polydimethylsiloxane) with embedded flexible chambers connecting a microfluidic system, thus realizing a morphological transformation for enhanced liquid repellency based on a nature-inspired rigid-flexible hybrid principle (i.e., triggering symmetry breaking and oscillator coupling mechanisms). The enhancement degree can be in situ tuned within around 300 ms owing to pneumatically controllable chamber morphologies. We also demonstrate that the surface can be freely programmed to achieve elaborated morphological pathways and gradients for preferred droplet manipulation such as directional rolling and bouncing. Our study highlights the potential of an in situ morphological transformation to realize tunable wettability and provides a programmable level of droplet control by intellectualizing conventional wetting materials.

INTRODUCTION

Artificially tailoring the wettability of surfaces, involving static and kinetic repellency, is an important goal in a wide range of scientific and technological fields including liquid-repelling,[1] anti-icing,[2] water collection,[3] energy harvesting,[4] and droplet manipulation.[5] Strong static repellency requires a successful suspension to bead up resting liquid droplets (contact angle > 150°) and tiny adhesion to enable droplet rolling (roll-off angle < 10°), which can be achieved by nature-inspired structural morphologies, for example, lotuses, roses, and springtails,[6,7] in marriage with low-surface-energy chemistry. Another two conditions should further apply for strong kinetic repellency against impacting droplets: Robust impalement resistance against droplet intrusion,[8] manifesting as droplet spreading,

Songtao Hu and Xiaobao Cao contributed equally to this study.

retracting, and eventual bouncing; and short droplet-surface contact time,[9] which usually includes spreading and retracting phases and is limited by the inertia-capillarity relationship.[10] Following the biomimetic pathway, plant leaves (e.g., *Nasturtium* and *Echeveria*) recommend convex morphologies on rigid microstructures (Supporting Information: Figure S1a) to redistribute the momentum and mass of impinging droplets and hence improve kinetic repellency.[11–15] Flexible butterfly wings further pave the way to elevating kinetic repellency by constructing surface-droplet oscillators in series (Supporting Information: Figure S1b), thereby shifting the research from statics to dynamics.[16–19]

Despite extensive progress in tailoring surface morphologies, nature also provides a higher level of biomimetic opportunities, with the intent to in situ tune wettability in response to external environments through a morphological transformation of surface structures, for example, the dry-wet reversible transformation of geckos,[20] tree frogs,[21] octopuses,[22] and springtails.[23] Although smart responsive materials with tunable physical properties in response to external stimuli, for example, chemical,[24] thermal,[25] magnetic,[26] and electric,[27] have emerged and come into use, they are mainly catalyzed (also limited) by progress in material science. In situ tailoring structural morphologies for wettability tuning independent of smart responsive materials remains elusive.

Here, we develop a pneumatic programmable superrepellent surface with the aid of a microfluidic technique.[28] Leveraging conventional wetting materials such as polydimethylsiloxane (PDMS), the microfluidics-endowed surface exhibits prescribed structural morphologies and controlled liquid repellency based on a nature-inspired rigid-flexible hybrid principle (i.e., symmetry breaking and oscillator coupling mechanisms) within around 300 ms. Also, the surface can be freely programmed to create elaborated morphological pathways and gradients so as to achieve preferred droplet manipulation such as directional rolling and bouncing. Our study highlights the potential of an in situ morphological transformation to realize tunable wettability and provides a programmable level of droplet control by intellectualizing conventional wetting materials.

RESULTS AND DISCUSSION

We developed a programmable superrepellent surface (Figure 1a) with each chamber enclosed by a flexible head, rigid sidewalls, and rigid substrate and connected to a microfluidic system. Theoretically, such chambers can provide reversible morphologies owing to a hydraulic or pneumatic control from the microfluidic system. These chambers can morph a prescribed convex curvature to trigger rigid-based enhancement on liquid repellency against droplet impact (Figure 1b).[11–15] Of note, a flexible principle can be also envisioned if the impacting pressure is higher than the pressure of the trapped medium inside the chambers so as to compress the convex chambers.[16–19] As the convex curvature can be adjusted by changing the input medium pressure, the above enhancement is expected to be in situ tuned. Besides the wettability tuning, with free chamber combination, it is possible to tailor a morphological pathway to drive resting droplets for directional rolling (Figure 1c),[29] or to create a morphological gradient to directionally rebound impacting droplets (Figure 1d).[30]

To realize our design, we used a standard soft lithography process (Supporting Information: Figure S2) to fabricate programmable superrepellent surfaces based on PDMS that consists of 4 × 5 square chambers (pitch $P = 5000\ \mu m$ and length $L = 4500\ \mu m$) as a prototype (Figure 2a). Each chamber was connected to an air-medium microfluidic system (Supporting Information: Figure S3) through microchannels, forming pneumatic control. These chambers were

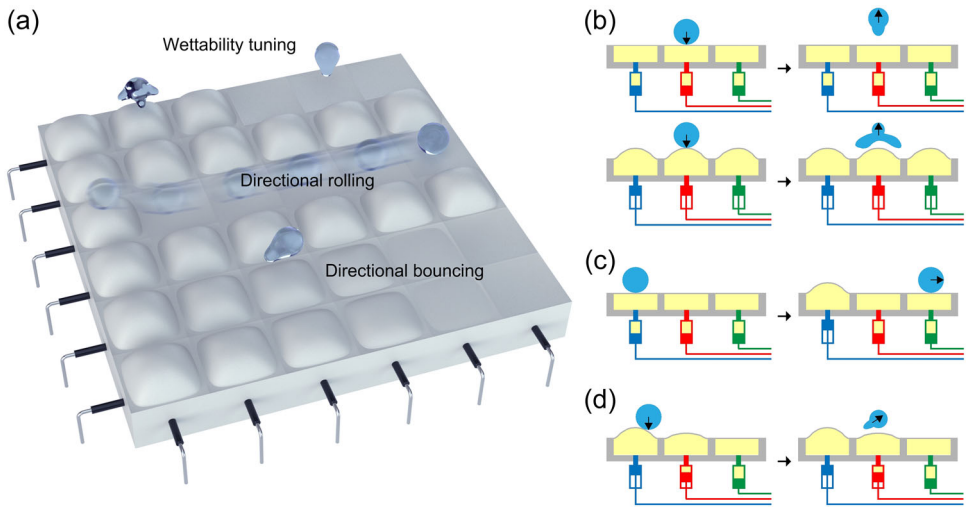

FIGURE 1 Pneumatic programmable superrepellent surfaces. (a) In marriage with microfluidics, morphologies of surface chambers are programmable for wettability tuning, directional rolling, and directional bouncing. (b) Schematics of programmable chambers to tune repellency against droplet impact. (c, d) Schematics of programmable chambers to achieve directional rolling of resting droplets and directional bouncing of impacting droplets.

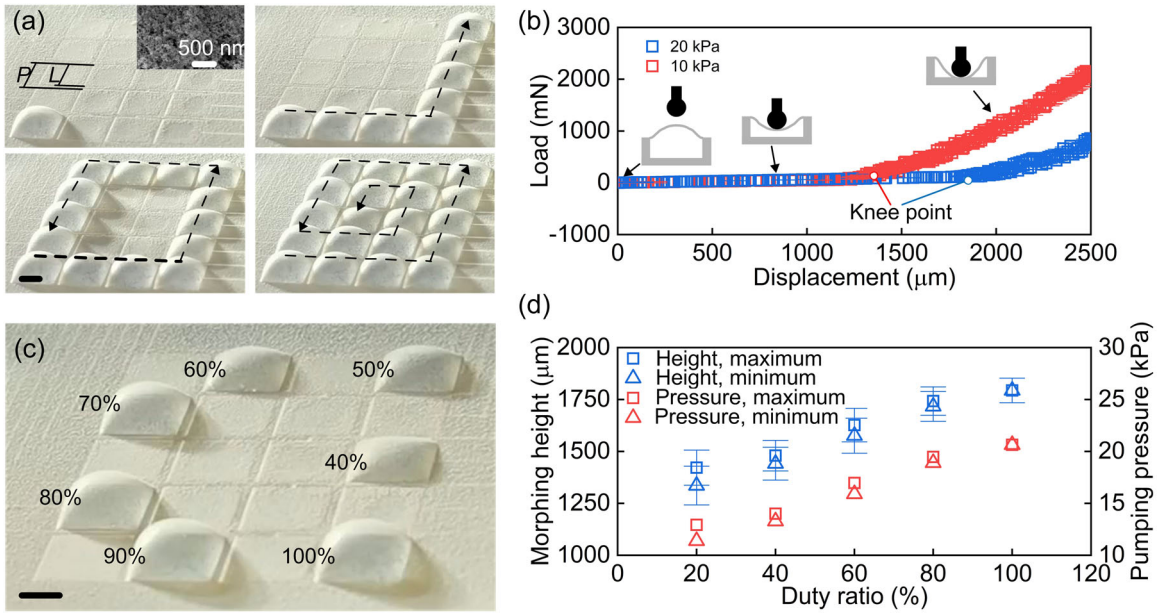

FIGURE 2 Mechanics of pneumatic programmable surfaces. (a) Enabling chambers from 0 to 20 kPa anticlockwise. (b) Load-displacement relationship of convex chambers under 10 and 20 kPa. (c) Different morphologies created on chambers from a single air source under 20 kPa through pulse-width modulation by changing the duty ratio from 100% to 40% clockwise. (d) Chamber morphing height as a function of duty ratio, as the rule to estimate pumping pressure for the pulse-width modulation under 20 kPa. Scale bars denote 2 mm.

tested in succession (Supporting Information: Movie S1), finding that the chambers arched to yield convex morphologies after air pumping. After turning off the pumps, the compressed air inside the chambers was released to balance with ambient pressure, resulting in morphological recovery. As the arching movements strongly relied on pumping pressure, we quantified the chamber morphing height as a function of pumping pressure (Supporting Information: Figure S4), confirming controllable morphologies endowed by the microfluidics. Also noteworthy was the occurrence of structural breakages on chamber heads when the pressure reached at 15 kPa (2000 and 3000 rpm) and 20 kPa (1000 rpm), which can be attributed to thin layer thickness (Supporting Information: Figure S5). Accordingly, we selected the value of 700 rpm as the spinning speed for fabricating chamber heads, as a trade-off between maximum morphing height (to maximize controlling range) and good durability. We also declined a spherical indenter to touch and compress the convex chambers under 10 and 20 kPa at the center, establishing the load-displacement relationship to quantify mechanics properties (Figure 2b). A knee point occurred at ~1200 μm under 10 kPa and ~1800 μm under 20 kPa in consistence with the chamber morphing heights (Supporting Information: Figure S4), thus grouping the load-displacement curve into two parts with the former for compressing chamber heads and the latter for compressing chamber heads and substrates.

We created different morphologies from a single air source (20 kPa) based on pulse-width modulation by changing the duty ratio, that is, the fraction of one period (50 ms) when a solenoid valve is open (Figure 2c; Supporting Information: Movie S2). As the duty ratio increased, the morphing height increased (Figure 2d). Of note, owing to the duty ratio, the chamber head periodically oscillated (Supporting Information: Figure S6), yielding maximum and minimum height values. Based on a polynomial fitting of the height-pressure function (Supporting Information: Figure S7), the 20-kPa pressure with a duty ratio of 80%, 60%, 40%, and 20% can be used to simulate ~19.2, ~16.4, ~13.6, and ~12.2 kPa, respectively.

For static repellency, the surfaces were moved upwards to touch hanging water droplets (Supporting Information: Figure S8 and Movie S3). When a nonchambered PDMS surface touched a droplet, the droplet was trapped by the surface of the microsyringe needle, exhibiting a contact angle of 113°. With low-surface-energy coatings, the nonchambered surface transferred into superhydrophobicity with a contact angle of 163° and a roll-off angle of 2°, beading up the droplet at the touching moment and preventing eventual droplet capture. Similarly, the droplet touched, beaded up, and left a pneumatic programmable surface under 0, 10, and 20 kPa. When the pneumatic programmable surface was lifted to compress the droplet, the droplet preferred to climb up along the needle rather than spreading over the surface, let alone compress the convex chamber, suggesting great static repellency in terms of high suspension and low adhesion. Such super repellency can be also evidenced by sliding the surfaces over hanging droplets (Supporting Information: Figure S9 and Movie S3).

We investigated kinetic repellency by impacting water droplets on the surfaces. For a pneumatic programmable surface, two extremely impacting positions were tested, i.e., the chamber center and the gap center within 2 × 2 chambers. Figure 3a shows the outcomes of impacting events along with an increased Weber number (*We*), which is nondimensionalized by $\rho D_0 V_0^2/\sigma$ to evaluate

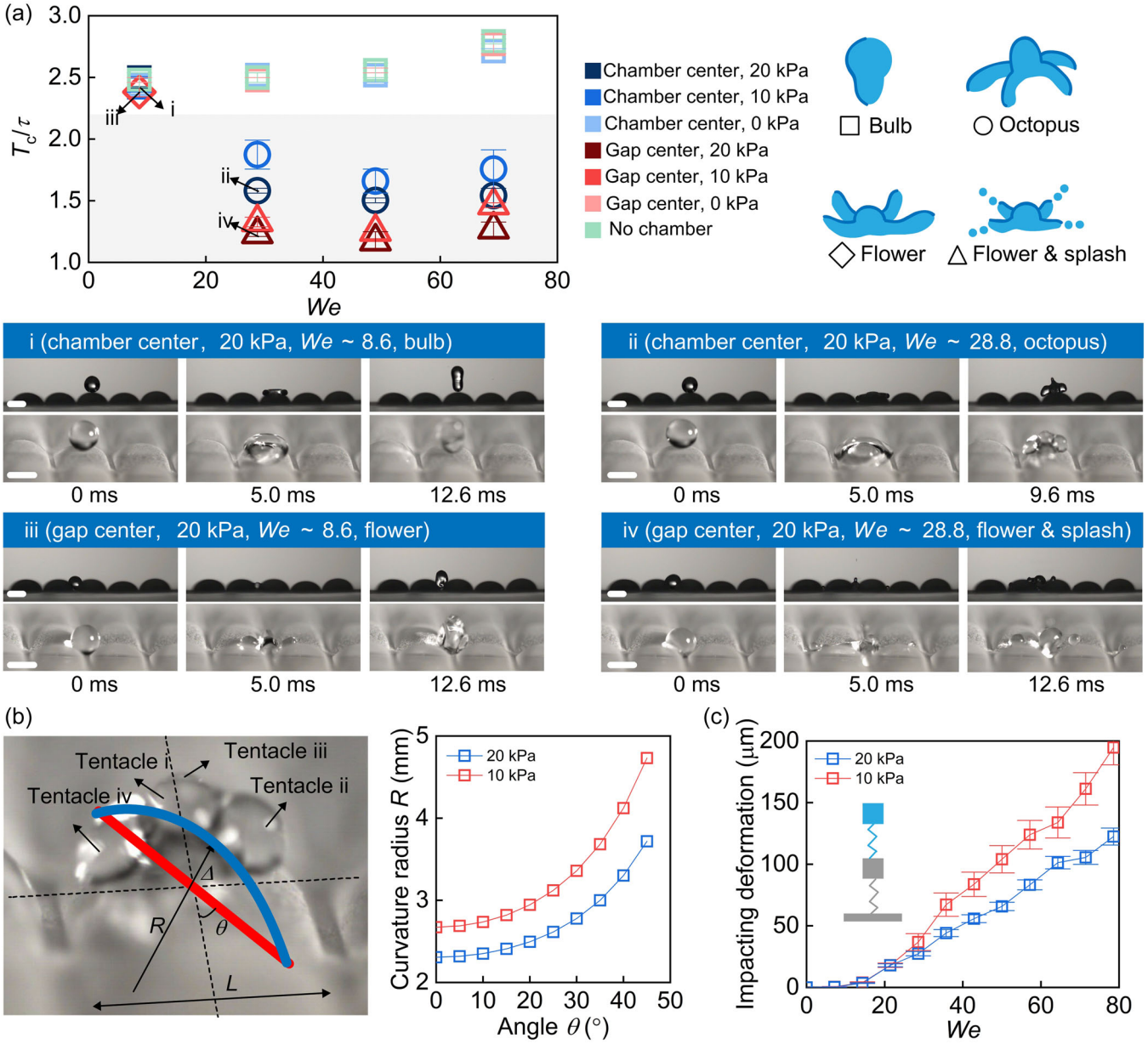

FIGURE 3 Repellency of pneumatic programmable surfaces against droplet impact. (a) Dimensionless contact time T_c/τ between a programmable surface (under 20, 10, and 0 kPa) and water droplets (with four impacting velocities denoted by Weber number [*We*] at 8.6, 28.8, 48.9, and 69.1), in comparison to a nonchambered surface as reference. Shadow denotes a theoretical limit of 2.2. Exemplary snapshots over time to visualize different bouncing postures in side and top views, including bulb (i), octopus (ii), flower (iii), and flower-splash (iv) configurations. (b) Theoretical analysis on calculating the curvature radius *R* of a convex chamber as a function of morphing height *Δ*, length *L*, and angle *θ*, positioning octopus tentacles. (c) Impacting deformation of convex chamber heads under 10 and 20 kPa as a function of *We*, suggesting a chamber-droplet oscillator coupling system. Scale bars denote 2 mm.

the ratio of inertial to capillary loads. D_0 and V_0 are the droplet diameter and velocity before impact; and ρ and σ are the droplet density and tension. Thanks to the low-surface-energy coating, only bouncing was observed with the absence of pinning, confirming robust impalement resistance against impacting pressure. We categorized the bouncing into four configurations as follows. For a nonchambered surface or a pneumatic programmable surface under 0 kPa, the droplet bounced off in a bulb-like shape. The pneumatic programmable surface with pumped air exhibited the same bulb-like bounce at *We* ~8.6 (Figure 3a, i) but started to transfer into an octopus-like bounce when *We* reached ~28.8 (Figure 3a, ii; Supporting Information: Movie S4), relating to the impact on chamber centers. In previous rigid liquid-repelling studies,[11–15] since the convex curvature only existed in a single direction, the bounced droplet presented an axisymmetric topology. Herein, as the convex curvature met a circular symmetry, four "tentacles" were generated in the directions with the maximum curvature (Figure 3b; Supporting Information: Note S1), yielding an octopus-like shape. Differently,

when the impact occurred on the gap centers at *We* ~8.6, the droplet spread along the four pathways between neighboring convex chambers and formed a flower-like bounce with four "petals" (Figure 3a, iii; Supporting Information: Movie S4). When *We* continued to rise up, the flower-like droplet started to eject satellites (Figure 3a, iv), resulting in splashing.[31]

As depicted in Figure 3a, *We* further explored how the contact time T_c was affected by the bouncing configurations, where τ is a timescale as $(0.125\,\rho D_0^3/\sigma)^{0.5}$.[10] The shadow denotes the theoretical limit value of 2.2 by balancing inertial and capillary loads. The nonchambered surface and the pneumatic programmable surface under 0 kPa exhibited contact time longer than the theoretical limit. At *We* ~8.6, owing to the bulb-like bounce, the droplets presented a similar contact time when they impacted the chamber centers under pressure. As *We* increased, the droplet impacted the chamber centers under 10 kPa and presented a reduced contact time in an octopus-like shape, even breaking through the theoretical limit, thus realizing our initial intention (Figure 1b). When the pumping pressure increased to 20 kPa, the contact time further reduced owing to a larger convex curvature, and even reached ~1.50 at *We* ~48.9, implying that the contact time reduction can be tuned by controlling pumping pressure. For the gap centers of the chambers under pressure, the contact time was also reduced (even reached ~1.17 at *We* ~48.9 under 20 kPa) due to flower-like bounce and can be controlled by changing pumping pressure. It can be concluded that the chambers of a pneumatic programmable surface can morph convex curvatures to trigger rigid-based (i.e., symmetry breaking) enhancement on liquid repellency against impacting droplets,[11–15] where the enhancement degree can be tuned based on the relationship between pumping pressure and morphing height.

As mentioned above (Figure 1b), a flexible liquid-repelling principle can be also envisioned if the impacting pressure is higher than the pressure of the air inside the chambers.[16–19] With a view to distinguishing the mechanism of contact time reduction, relying on the conservation of momentum and energy,[32] we established a theoretical model (Supporting Information: Figure S10 and Note S2) to estimate the maximum impacting load. When *We* increased from 8.6 to 69.1, the maximum impacting load without any eccentricity increased from 1.2 to 9.7 mN (Supporting Information: Figure S11). Accordingly, we extracted the load-displacement curves (Figure 2b) in the range of 0 to 10 mN (Supporting Information: Figure S12), implying that the convex chamber under 10 and 20 kPa had a downward deformation of ~160 and ~105 μm at *We* ~69.1 (Figure 3c) which has suggested the existence of the flexible principle. Accordingly, we established a chamber-droplet oscillator coupling model (Figure 3c; Supporting Information: Note S3).[17] Given the natural frequency of the system, the contact time and impacting deformation showed a clear relationship to impacting velocity (Supporting Information: Figure S13), implying the secondary role played by the flexible principle in comparison to the rigid one. Also, the octopus-like bounce, rather than pancake-like bounce,[33] has again highlighted the dominant role played by the rigid principle. Of course, it is possible to increase the proportion of the flexible principle by selecting soft materials with more stretchable properties.[34] Yet, extreme compliance is easy to thoroughly change the convex morphologies of the chambers, making the liquid-repelling mechanism more complex.

Besides the wettability tuning above, we gauged the droplet manipulating capacity of our pneumatic programmable surfaces (Figure 1c, d). By enabling the underlying chamber from 0 to 20 kPa, a resting droplet was driven by the morphing chamber head and entered into a directional rolling (Figure 4a; Supporting Information: Movie S5). As the morphing period was around 300 ms, the droplet was lifted slowly, avoiding a selfpropelling bounce that can be induced by environmental changes[2] and droplet coalescence.[35] Such a directional rolling can steer the original direction by another morphing chamber. With regard to impacting droplets, the convex chamber under 20 kPa exhibited a directional

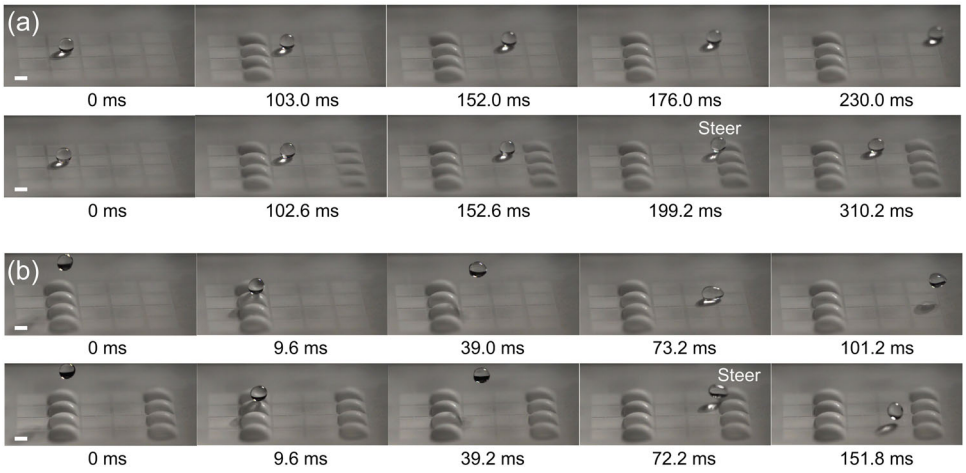

FIGURE 4 Droplet manipulating capacity of pneumatic programmable surfaces. (a) Directional rolling of resting droplets and direction steering. (b) Directional bouncing of impacting droplets at Weber number (*We*) ~8.6 and direction steering. Scale bars denote 2 mm.

bouncing response (Figure 4b; Supporting Information: Movie S6), whose direction can be steered by enabling another chamber. However, the morphing period (~300 ms) is longer than the time interval between two successive bounces, thus requiring a pre-enabling chamber operation for direction steering that restricts the programmable level. A thorough study on structure optimization and material selection may further reduce the morphing period,[34] but may lead to another challenge in the directional rolling (i.e., triggering a selfpropelling bounce to generate instability).

Based on the droplet manipulating capacity above, our surface was pneumatically programmed to generate a morphological pathway (route chambers under 0 kPa and surrounding chambers under 20 kPa) to prescribe a certain rolling route (e.g., along *X* direction), along which a resting droplet directionally rolled and eventually mixed with another resting droplet (Figure 5a; Supporting Information: Movie S7), implying the potential of droplet mixture in bioreaction. Also, we pumped the chambers under 20, 15, 10, 5, and 0 kPa to create a morphological gradient on the surface to prescribe the bouncing direction (e.g., along *X* direction). Whether the impact occurred on the left or the right side of a chamber, the droplet exhibited a rightward bounce eventually (Figure 5b; Supporting Information: Movie S8). Besides the one-dimensional droplet control above, in marriage between morphological pathways and gradients, we pumped the chambers under 20, 15, 10, 5, and 0 kPa to create a river-valley-like morphology for two-dimensional directional (i.e., *X* and *Y* directions) rolling and bouncing. A resting droplet was driven by a morphing chamber from 0 to 20 kPa, rolled along the river valley but eventually stopped at the corner due to energy dissipation (Figure 5c; Supporting Information: Movie S9). Differently, a droplet impacted a morphing chamber under 20 kPa and had higher kinetic energy, resulting in a successful trampolining throughout the river valley.

CONCLUSION

In summary, nature has inspired various structural morphologies for artificial surfaces, leading to extensive progress in tailoring wettability. However, nature also provides another level of biomimetic intents to in situ tune wettability through a morphological transformation. In contrast to smart responsive materials that are catalyzed (also limited) by progress in material science, we bridged the gap between two research realms of functional surfaces and microfluidics to tailor conventional wetting materials (e.g., PDMS), yielding a pneumatic programmable surface with 300-ms response time. The surface was shown to improve liquid repellency by reducing liquid-surface contact time based on a nature-inspired rigid-flexible hybrid principle (i.e., symmetry breaking and oscillator coupling mechanisms), where the enhancement degree can be in situ tuned owing to pneumatically controllable chamber morphologies. Moreover, the surface was shown to be freely programmed to create elaborated morphologies for preferred droplet manipulation such as directional rolling and bouncing. From a biological perspective, our study highlights the potential of an in situ morphological transformation for wettability tuning and provides a programmable level of droplet control by intellectualizing conventional wetting materials.

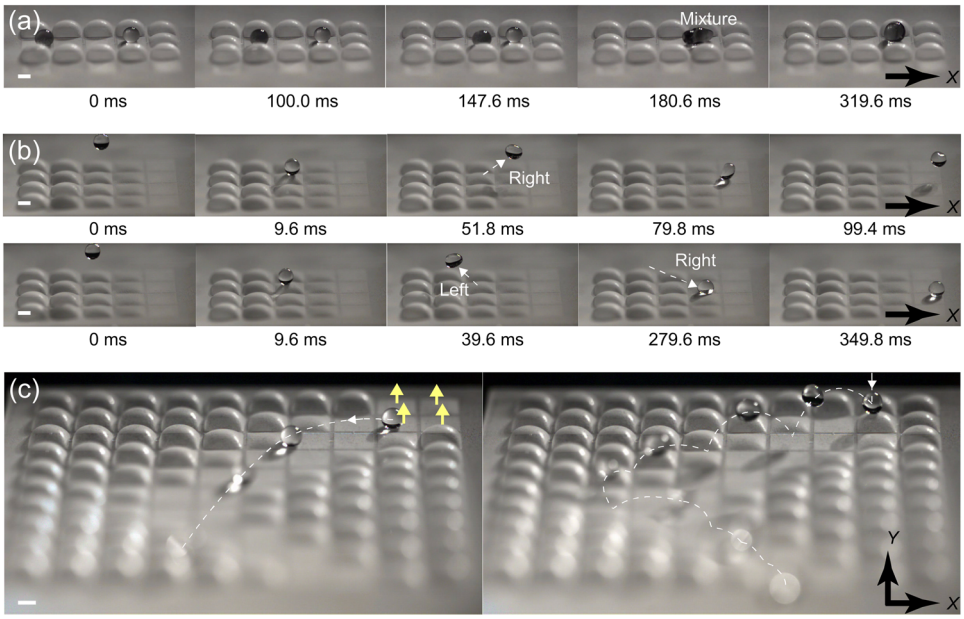

FIGURE 5 Droplet manipulating applications of pneumatic programmable surfaces. (a) One-dimensional directional rolling of resting droplets programmed by a morphological pathway to trigger droplet mixture. (b) One-dimensional directional bouncing of impacting droplets at Weber number (*We*) ~8.6 programmed by a morphological gradient. (c) Two-dimensional directional rolling and bouncing (at *We* ~8.6) programmed by a river-valley-like morphology. Yellow arrows denote morphing behaviors of chambers from 0 to 20 kPa. White arrows denote motion track of droplets. Scale bars denote 2 mm.

METHODS

A silicon wafer was heated on a 200°C hotplate for 10 min. A 2-mL SU-8 photoresist (MicroChem, Germany) was poured on the wafer and spun at 3000 rpm for 30 s. The wafer was heated at 65°C for 5 min and at 95°C for 10 min. The wafer after cooling was exposed to a strength of 5.6 mW cm^{-2} for 43 s. The exposed wafer was heated at 95°C for 10 min and developed by a SU-8 developer (MicroChem). The wafer was dried at 200°C for 10 min to heal the SU8 structures and enhance the stickiness between the SU8 and the wafer.

Sylgard-184 PDMS was mixed in a 10:1 weight ratio and placed in a vacuum desiccator for a 20-min degassing. The degassed PDMS was poured on the microfluidic mold and heated at 80°C for 2h. The degassed PDMS was also poured on a silanized silicon wafer, spun at a certain speed (300–3000 rpm) for 2 min, and then heated at 80°C for 2 h. The thick PDMS layer on the mold was peeled off and punched holes at the inlets of microchannels. The thick PDMS layer was plasma treated for 16 s and balanced for 90 s in a vacuum environment together with the thin PDMS layer on the silanized silicon wafer. The thick PDMS layer was bonded to the thin layer and peeled off after 2-h heating at 80°C. Commercial low-surface-energy particles Ultra-Ever Dry (Ultra Tech International Inc) were coated.[13,30]

Morphological images of pneumatic programmable surfaces were taken with an optical microscope LW300LMDT (Cewei Guangdian) and a scanning electron microscope Sirion 200 (Philips).

The chambers were pumped under 20 kPa in succession to confirm the morphological transformation of pneumatic programmable surfaces. To quantify the relationship between morphing height and pumping pressure, the chambers were enabled under 2.5, 5, 7.5, 10, 15, and 20 kPa, respectively. The morphing behaviors of chambers were captured by a camera 5KF10 (FuHuang AgileDevice) at a rate of 64 fps. Pulse-width modulation method was conducted to generate different chamber morphologies from a single air source under 20 kPa. For a certain chamber, the duty ratio was changed from 100%, 80%, 60%, 40% to 20%. Then, for a pneumatic programmable surface, seven chambers were set to different duty ratio values of 100%, 90%, 80%, 70%, 60%, 50%, and 40%, respectively. The morphing behaviors of chambers were recorded by the camera at a rate of 5000 fps.

The surfaces were lifted up to touch hanging deionized water droplets in a volume of 2-μL on a contact angle goniometer SDC-100 (SINDIN) in sessile drop mode under controlled temperature (25°C) and relative humidity (45%). Also, the surfaces were horizontally moved to slide over hanging water droplets. To quantify, the contact angle was measured 30 s after the droplets contacted the surfaces to ensure equilibrium. The roll-off angle was captured by tilting the surface platform to record the tilting angle when resting droplets started to roll. The measurement was repeated three times.

An electrically controlled microsyringe pump was used to generate and release 8-μL deionized water droplets at a specified height (*We* ~8.6, ~28.8, ~48.9, and ~69.1). The impacting position was adjusted by horizontally moving the surface platform in relation to the microsyringe. Impacting behaviors were recorded by the camera at a rate of 5000 fps. The measurement was repeated three times.

A spherical indenter was declined to touch and compress the convex chambers under 10 and 20 kPa at the center on a tensile-pressure tester ZQ990A (ZHIQU Precision Instruments) in pressure mode. For a certain displacement, the corresponding load between the indenter and the chamber was recorded, establishing the load-displacement relationship. The measurement was repeated three times.

To drive resting water droplets and steer rolling direction, the target chambers were enabled from 0 to 20 kPa. To directionally rebound and steer bouncing direction of impacting water droplets at *We* ~8.6, the target chambers were pumped under 20 kPa. For one-dimensional directional rolling, a morphological pathway was created by supplying air pressure under 20 and 0 kPa. For one-dimensional directional bouncing, a morphological gradient was created by supplying air pressure under 20, 15, 10, 5, and 0 kPa. A pneumatic programmable surface with 10 × 10 chambers was pumped under 20, 15, 10, 5, and 0 Pa to yield a river-valley-like morphology. Two-dimensional directional rolling (enabled from 0 to 20 kPa) and bouncing (pumped under 20 kPa and released at *We* ~8.6) tests were conducted. The behaviors were recorded by the camera at a rate of 5000 fps.

ACKNOWLEDGMENTS

This study was supported by National Natural Science Foundation of China, grant 12002202 (Songtao Hu), Young Elite Scientist Sponsorship Program by the China Association for Science and Technology, grant YESS20200403 (Songtao Hu), National Natural Science Foundation of China, grant 12121002 (Zhike Peng), and State Key Laboratory of Mechanical System and Vibration, grant MSVZD202104 (Songtao Hu).

CONFLICT OF INTEREST

The authors declare no conflict of interest.

ETHICS STATEMENT

Hereby, we consciously assure that for the manuscript Pneumatic Programmable Superrepellent Surfaces the following is fulfilled:

(1) This material is the authors' own original work, which has not been previously published elsewhere.
(2) The paper is not currently being considered for publication elsewhere.
(3) The paper reflects the authors' own research and analysis in a truthful and complete manner.
(4) The paper properly credits the meaningful contributions of coauthors and co-researchers.
(5) The results are appropriately placed in the context of prior and existing research.
(6) All sources used are properly disclosed (correct citation). Literally copying of text must be indicated as such by using quotation marks and giving proper reference.

(7) All authors have been personally and actively involved in substantial work leading to the paper and will take public responsibility for its content.

ORCID

Songtao Hu http://orcid.org/0000-0002-8405-3788

REFERENCES

1. Liu T, Kim CJ. Turning a surface superrepellent even to completely wetting liquids. *Science*. 2014;346(6213):1096-1100.
2. Schutzius TM, Jung S, Maitra T, Graeber G, Kohme M, Poulikakos D. Spontaneous droplet trampolining on rigid superhydrophobic surfaces. *Nature*. 2015;527:82-85.
3. Zhang X, Sun L, Wang Y, Bian F, Wang Y, Zhao Y. Multibioinspired slippery surfaces with wettable bump arrays for droplets pumping. *Proc Natl Acad Sci USA*. 2019;116(42):20863-20868.
4. Xu W, Zheng H, Liu Y, et al. A droplet-based electricity generator with high instantaneous power density. *Nature*. 2020;578:392-396.
5. Sun L, Bian F, Wang Y, Wang Y, Zhang X, Zhao Y. Bioinspired programmable wettability arrays for droplets manipulation. *Proc Natl Acad Sci USA*. 2020;117(9):4527-4532.
6. Hensel R, Neinhuis C, Werner C. The springtail cuticle as a blueprint for omniphobic surfaces. *Chem Soc Rev*. 2016;45(2):323-341.
7. Tuteja A, Choi W, Ma M, et al. Designing superoleophobic surfaces. *Science*. 2007;318(5856):1618-1622.
8. Yun G-T, Jung W-B, Oh MS, et al. Springtail-inspired super-omniphobic surface with extreme pressure resistance. *Sci Adv*. 2018;4(8):eaat4978.
9. Vasileiou T, Schutzius TM, Poulikakos D. Imparting icephobicity with substrate flexibility. *Langmuir*. 2017;33(27):6708-6718.
10. Richard D, Clanet C, Quere D. Contact time of a bouncing drop. *Nature*. 2002;417:811.
11. Hu S, Reddyhoff T, Puhan D, et al. Droplet manipulation of hierarchical steel surfaces using femtosecond laser fabrication. *Appl Surf Sci*. 2020;521:146474.
12. Song M, Liu Z, Ma Y, Dong Z, Wang Y, Jiang L. Reducing the contact time using macro anisotropic superhydrophobic surfaces—effect of parallel wire spacing on the drop impact. *NPG Asia Mater*. 2017;9:e415.
13. Gauthier A, Symon S, Clanet C, Quere D. Water impacting on superhydrophobic macrotextures. *Nat Commun*. 2015;6:8001.
14. Liu Y, Andrew M, Li J, Yeomans JM, Wang Z. Symmetry breaking in drop bouncing on curved surfaces. *Nat Commun*. 2015;6:10034.
15. Bird JC, Dhiman R, Kwon H, Varanasi KK. Reducing the contact time of a bouncing drop. *Nature*. 2013;503:385-388.
16. Hu S, Cao X, Reddyhoff T, et al. Liquid repellency enhancement through flexible microstructures. *Sci Adv*. 2020;6(32):eaba9721.
17. Chantelot P, Coux M, Clanet C, Quere D. Drop trampoline. *EPL*. 2018;124(2):24003.
18. Wang L, Gong Q, Zhan S, Jiang L, Zheng Y. Robust anti-icing performance of a flexible superhydrophobic surface. *Adv Mater*. 2016;28(35):7729-7735.
19. Vasileiou T, Gerber J, Prautzsch J, Schutzius TM, Poulikakos D. Superhydrophobicity enhancement through substrate flexibility. *Proc Natl Acad Sci USA*. 2016;113(47):13307-13312.
20. Stark AY, Badge I, Wucinich NA, Sullivan TW, Niewiarowski PH, Dhinojwala A. Surface wettability plays a significant role in gecko adhesion underwater. *Proc Natl Acad Sci USA*. 2013;110(116):6340-6345.
21. Drotlef DM, Blumler P, del Campo A. Magnetically actuated patterns for bioinspired reversible adhesion (dry and wet). *Adv Mater*. 2014;26(5):775-779.
22. Baik S, Kim DW, Park Y, Lee T-J, Bhang SH, Pang C. A wet-tolerant adhesive patch inspired by protuberances in suction cups of octopi. *Nature*. 2017;546:396-400.
23. Liu X, Gu H, Ding H, et al. 3D bioinspired microstructures for switchable repellency in both air and liquid. *Adv Sci*. 2020;7(20):2000878.
24. Lahann J, Mitragotri S, Tran TN, et al. A reversibly switching surface. *Science*. 2003;299(5605):371-374.
25. Sun T, Wang G, Feng L, et al. Reversible switching between superhydrophilicity and superhydrophobicity. *Angew Chem Int Ed*. 2004;43(3):357-360.
26. Jiang S, Hu Y, Wu H, et al. Multifunctional Janus microplates arrays actuated by magnetic fields for water/light switches and bio-inspired assimilatory coloration. *Adv Mater*. 2019;31(15):1807507.
27. Li Y, Li J, Liu L, et al. Switchable wettability and adhesion of micro/nanostructured elastomer surface via electric field for dynamic liquid droplet manipulation. *Adv Sci*. 2020;7(18):2000772.
28. Thorsen T, Maerkl SJ, Quake SR. Microfluidic large-scale integration. *Science*. 2002;298(5593):580-584.
29. Yu J, Wei X, Guo Y, et al. Self-powered droplet manipulation system for microfluidics based on triboelectric nanogenerator harvesting rotary energy. *Lab Chip*. 2021;21(2):284-295.
30. Sun Q, Wang D, Li Y, et al. Surface charge printing for programmed droplet transport. *Nat Mater*. 2019;18:936-941.
31. Liu Q, Lo JHY, Li Y, Liu Y, Zhao J, Xu L. The role of drop shape in impact and splash. *Nat Commun*. 2021;12:3068.
32. Soto D, De Lariviere AB, Boutillon X, Clanet C, Quere D. The force of impacting rain. *Soft Matter*. 2014;10(27):4929-4934.
33. Liu Y, Moevius L, Xu X, Qian T, Yeomans JM, Wang Z. Pancake bouncing on superhydrophobic surfaces. *Nat Phys*. 2014;10(7):515-519.
34. Baumgartner R, Kogler A, Stadlbauer JM, et al. A lesson from plants: High-speed soft robotic actuators. *Adv Sci*. 2020;7(5):1903391.
35. Liu J, Guo H, Zhang B, et al. Guided self-propelled leaping of droplets on a micro-anisotropic superhydrophobic surface. *Angew Chem Int Ed*. 2016;55(13):4265-4269.

SUPPORTING INFORMATION

Additional supporting information can be found online in the Supporting Information section at the end of this article.

How to cite this article: Hu S, Cao X, Reddyhoff T, et al. Pneumatic programmable superrepellent surfaces. *Droplet*. 2022;1:53-60. doi:10.1002/dro2.11